

Supplemental material

1. The ocean dynamic model and comparison with observations

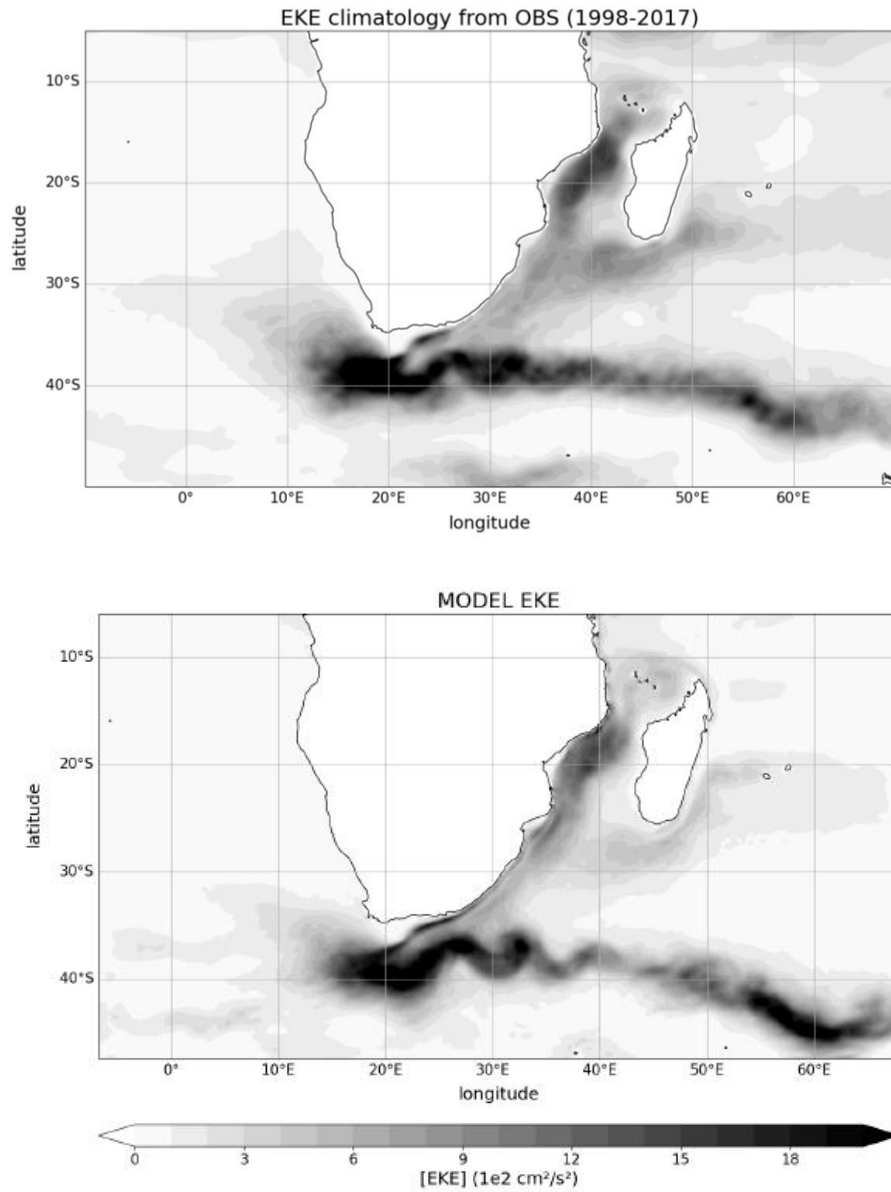


Figure S1. Annual climatology of eddy kinetic energy (EKE) from (top) AVISO observations and (bottom) the SWAG122 model, both calculated over the same 20-year period (1998-2017).

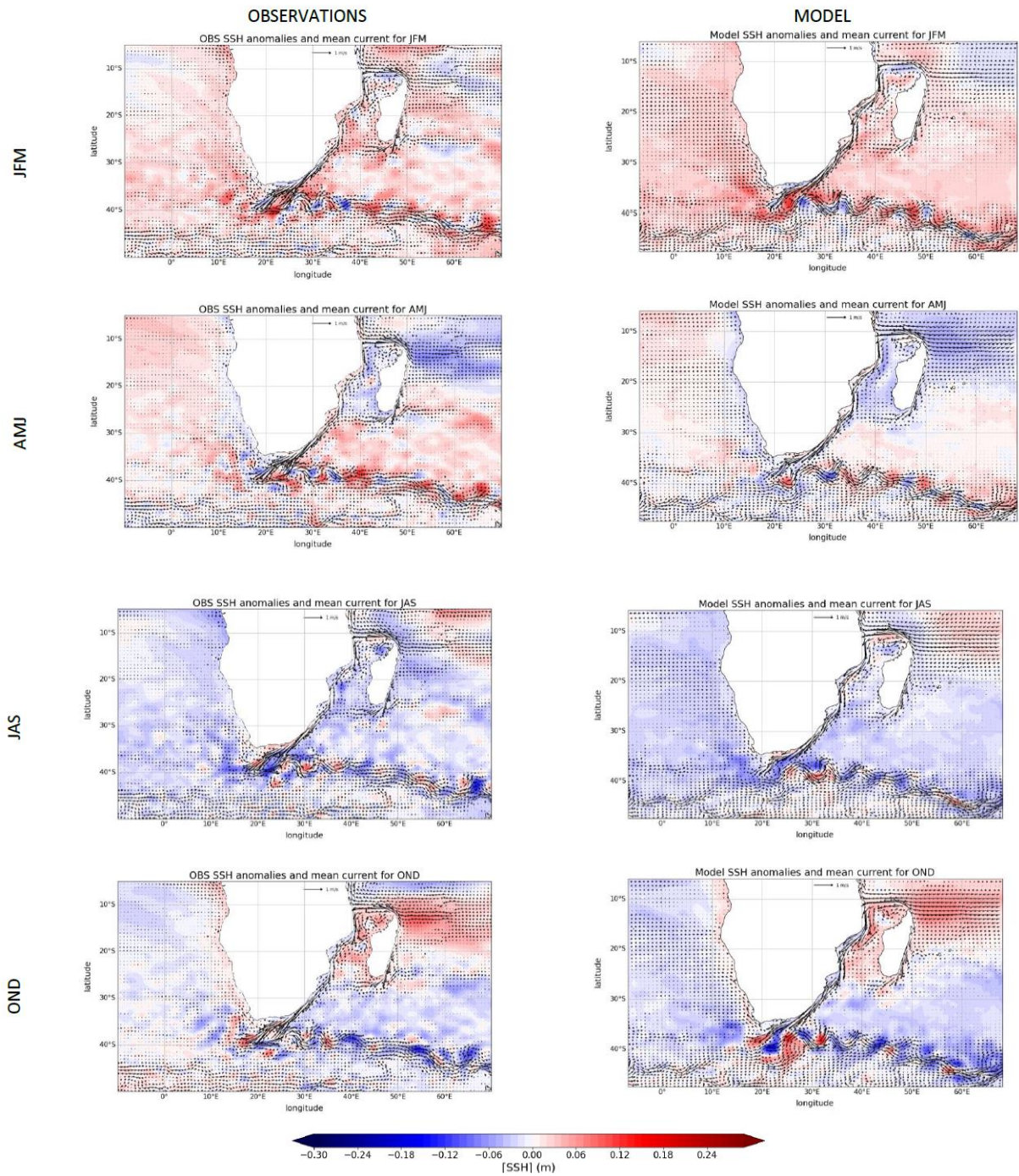


Figure S2. Seasonal climatology of sea surface height (SSH, colored map) and surface velocity (black arrows) from AVISO observations (left column) and the SWAG122 model (right column), both calculated over the same 20-year period (1998-2017). Seasonal averages correspond to three-month averages with JFM January-February-March, AMJ April-May-June, JAS July-August-September and OND October-November-December.

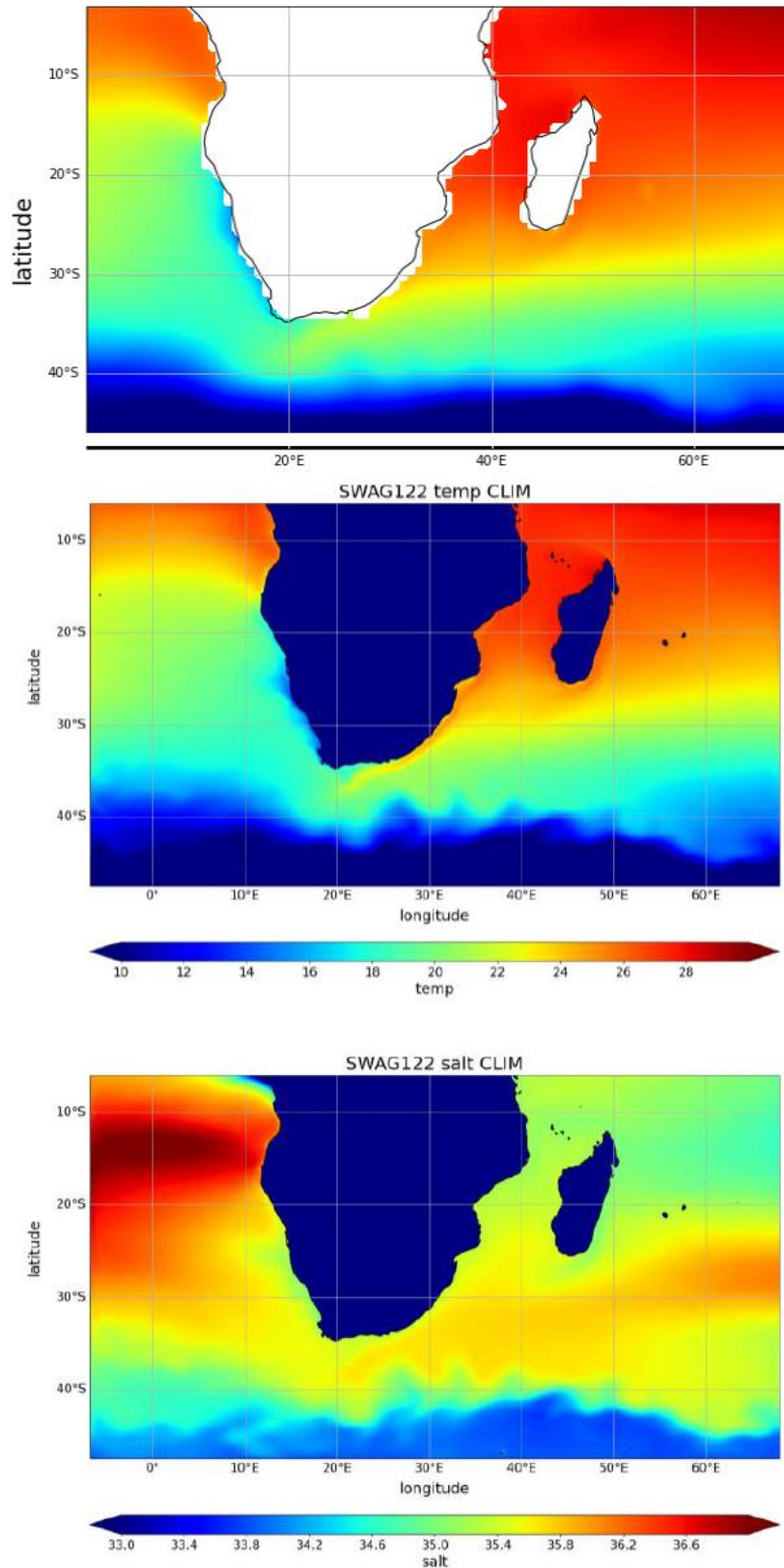


Figure S3. Surface temperature (top 2 figures sharing the same color bar) from ERA-5 reanalysis (1st row) and model (2nd row), and surface salinity (3rd row) from SWAG122 (averaged over 20 years - 1998-2017).

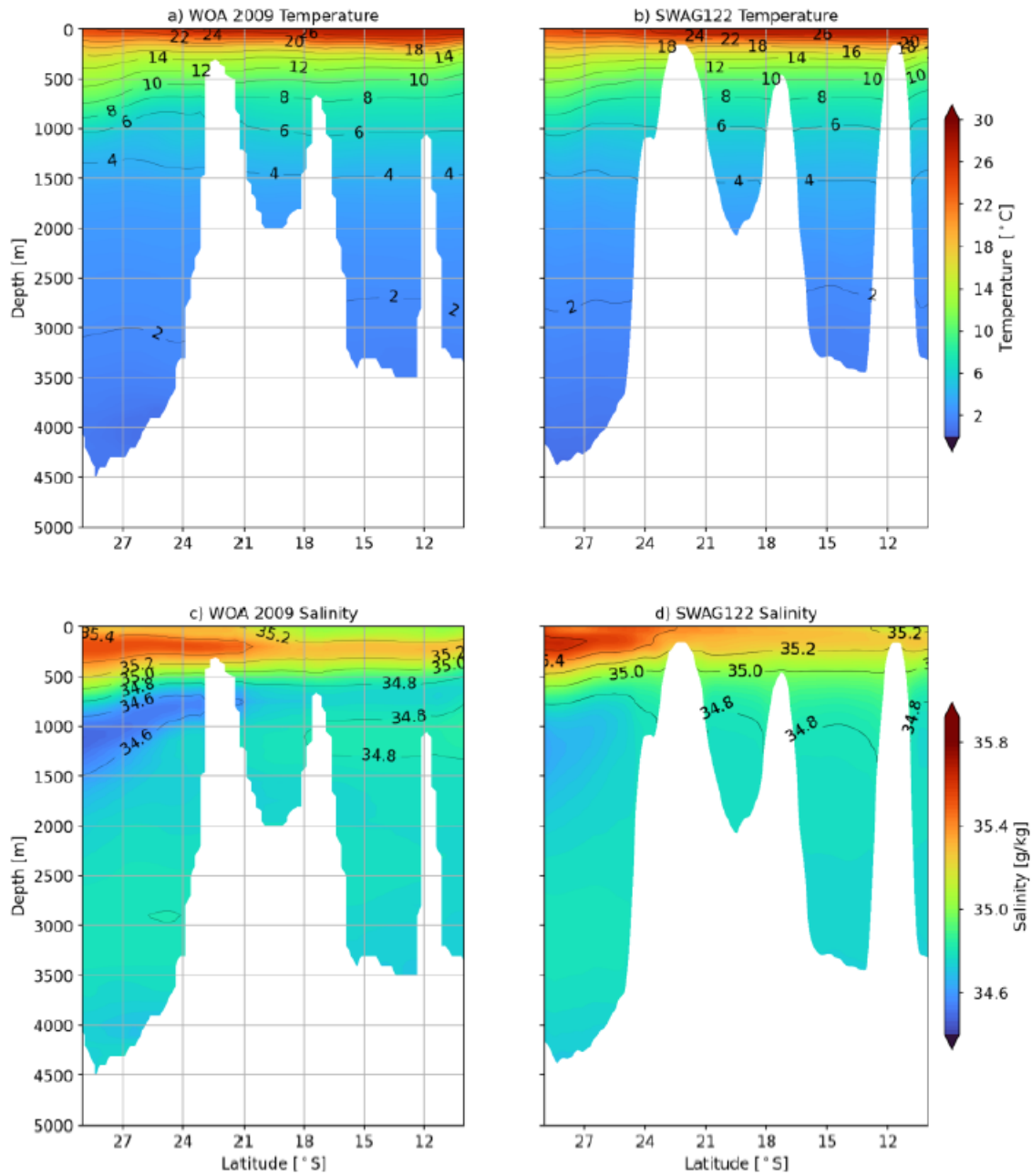


Figure S4. Comparison between World Ocean Atlas (WOA2018, left column), and SWAG122 (20-year average - right column) for temperature (top) and salinity (bottom) at 41°E.

2. The biogeochemical model and comparison with observations

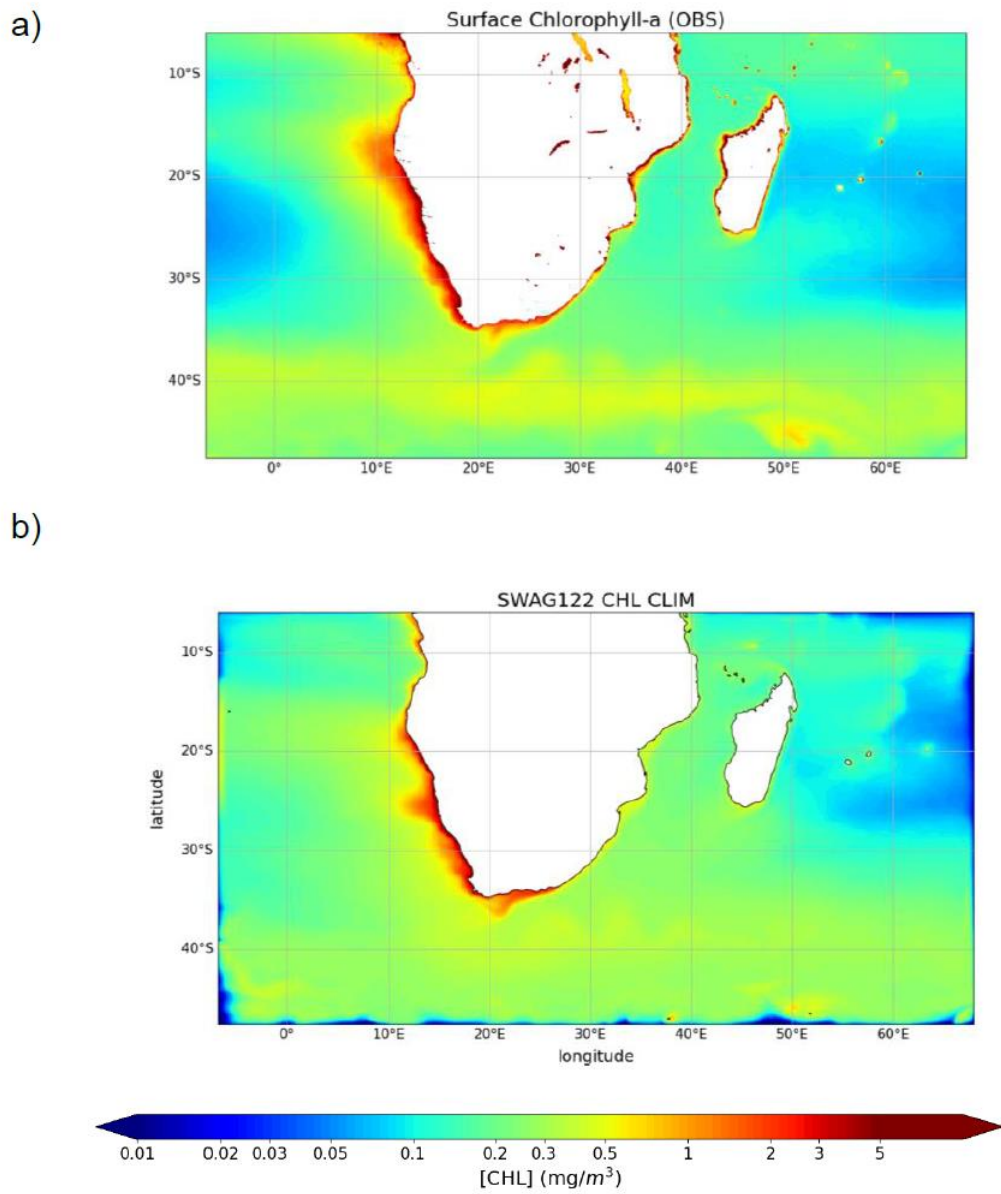


Figure S5. Surface chlorophyll-a concentration averaged over the available period for (a) observations and (b) SWAG122 (over 20 years - 1998-2017).

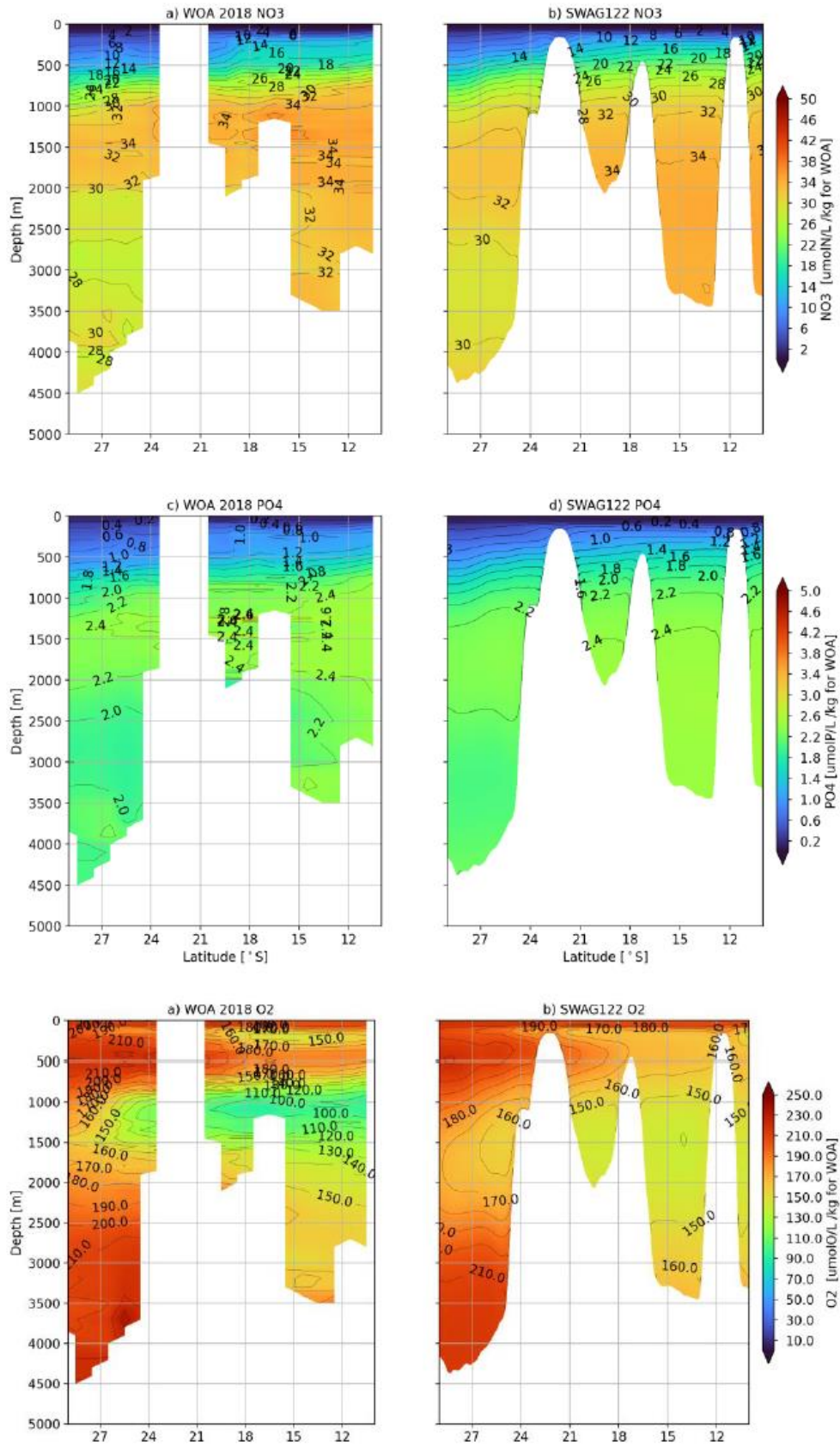


Figure S6. Comparison between World Ocean Atlas (WOA2018, left column), and SWAG122 (20-year average - right column) for NO₃ (top – a, b) PO₄ (middle, c, d) and O₂ (bottom, e, f) at 41°E.

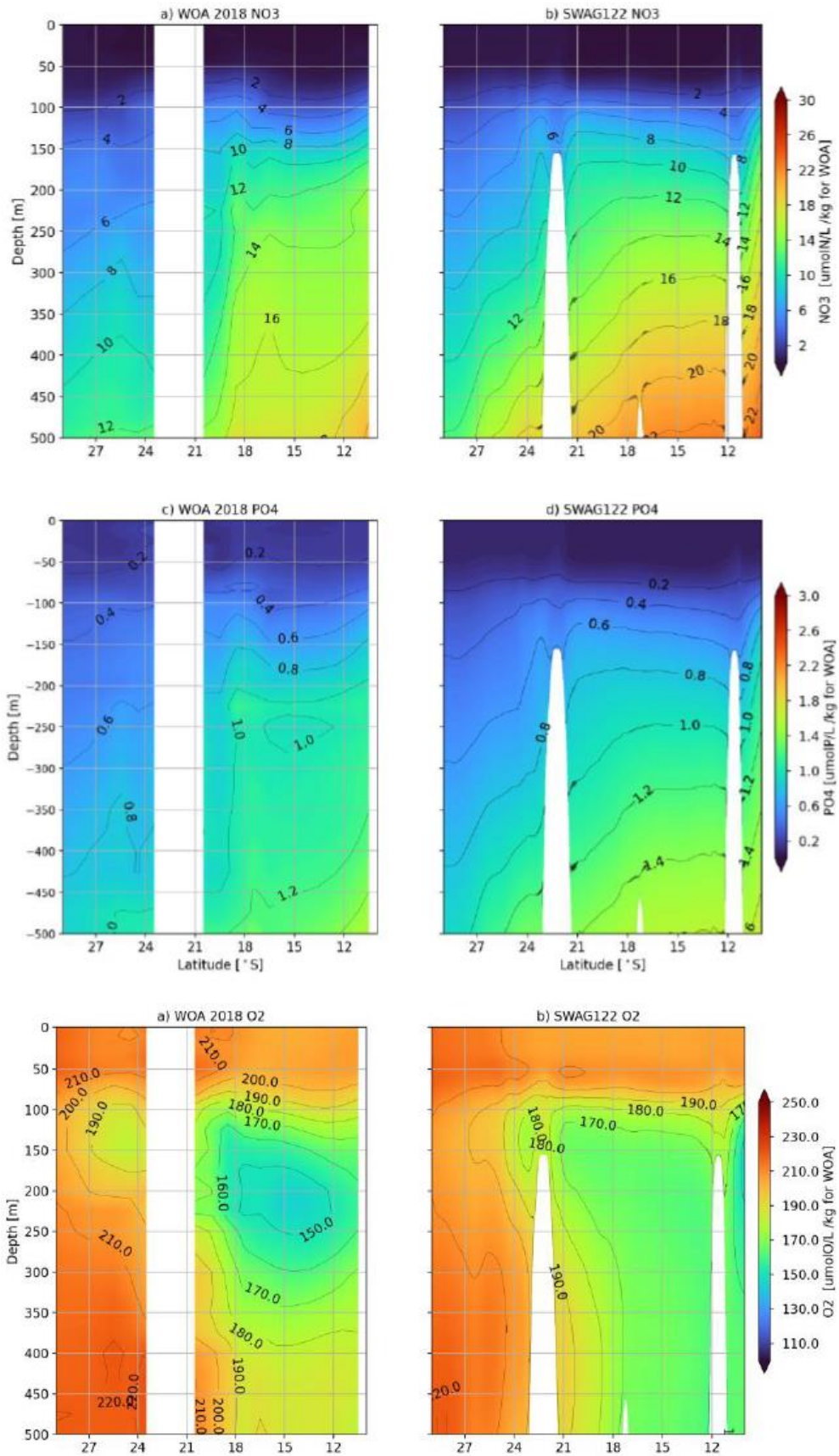


Figure S7. Same as Figure S6 zoomed from 0 to 500m depth.

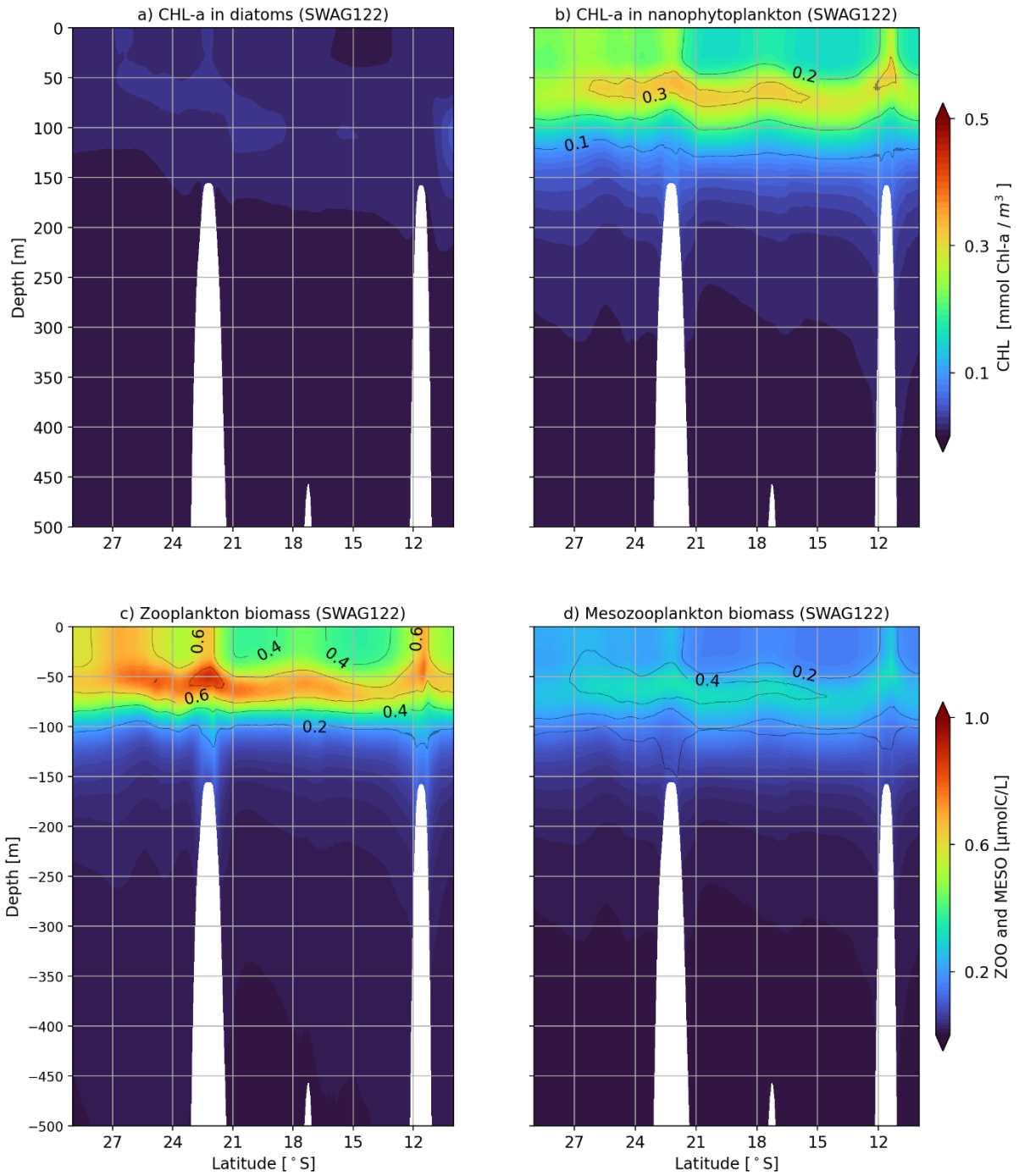


Figure S8. Yearly climatology of SWAG122 outputs (20-year average) at 41°E for Chl-a in diatoms (a), Chl-a in nanophytoplankton (b), Zooplankton (c) and Meso zooplankton (d).

3. The biogeochemical model: seasonal climatologies

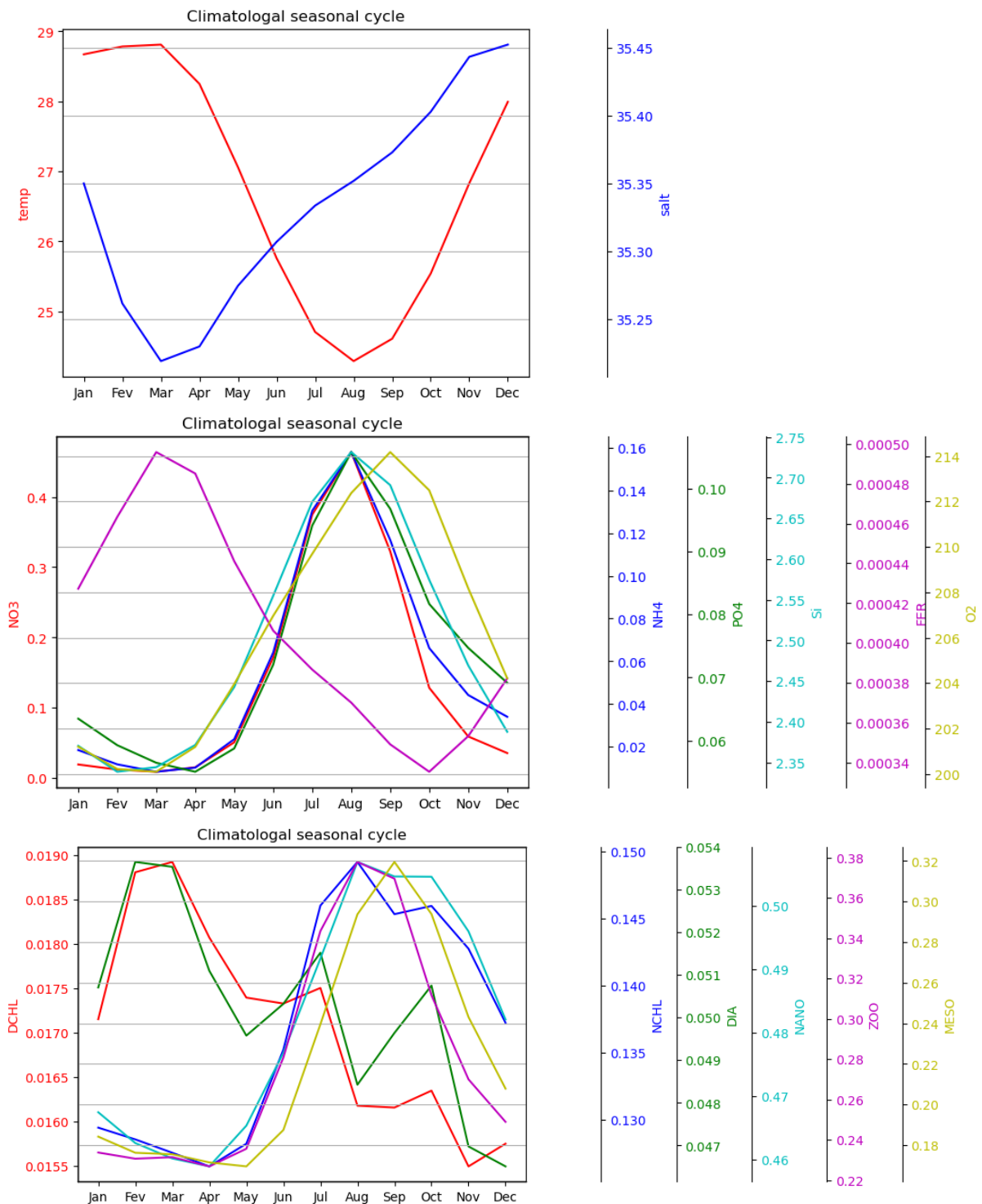


Figure S9. Monthly climatology averaged over the Mozambique Channel (from 25°S to 12.5°S) for physical tracers (temperature and salinity on top), for nutrients (in the middle), and for planktonic components (bottom). Units are the same as in FigS9 to S13.

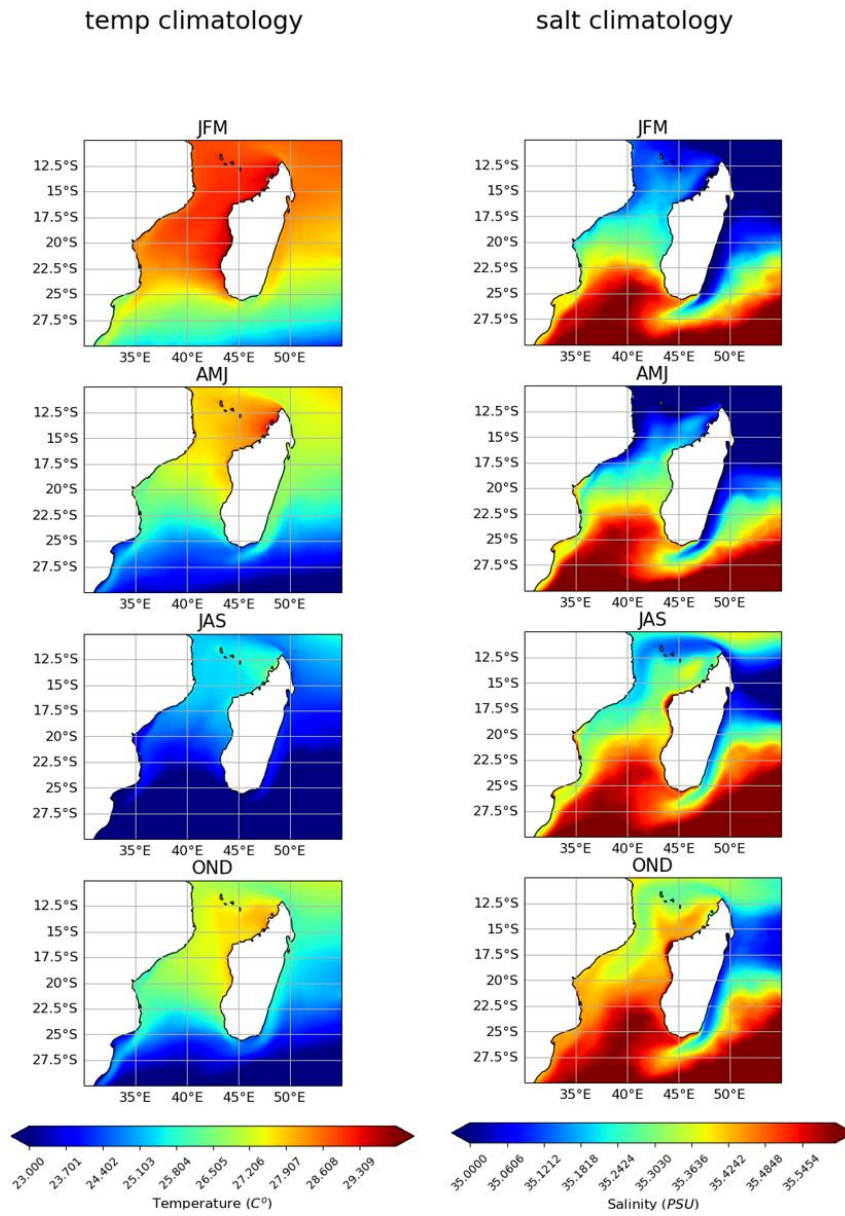


Figure S10. Seasonal evolution of surface temperature (left) and surface salinity (right). JFM, AMJ, JAS, and OND refer to seasonal averages of January-February-March, April-May-June, July-August-September, and October-November-December, respectively.

NO3 climatology

NH4 climatology 0-200m

PO4 climatology

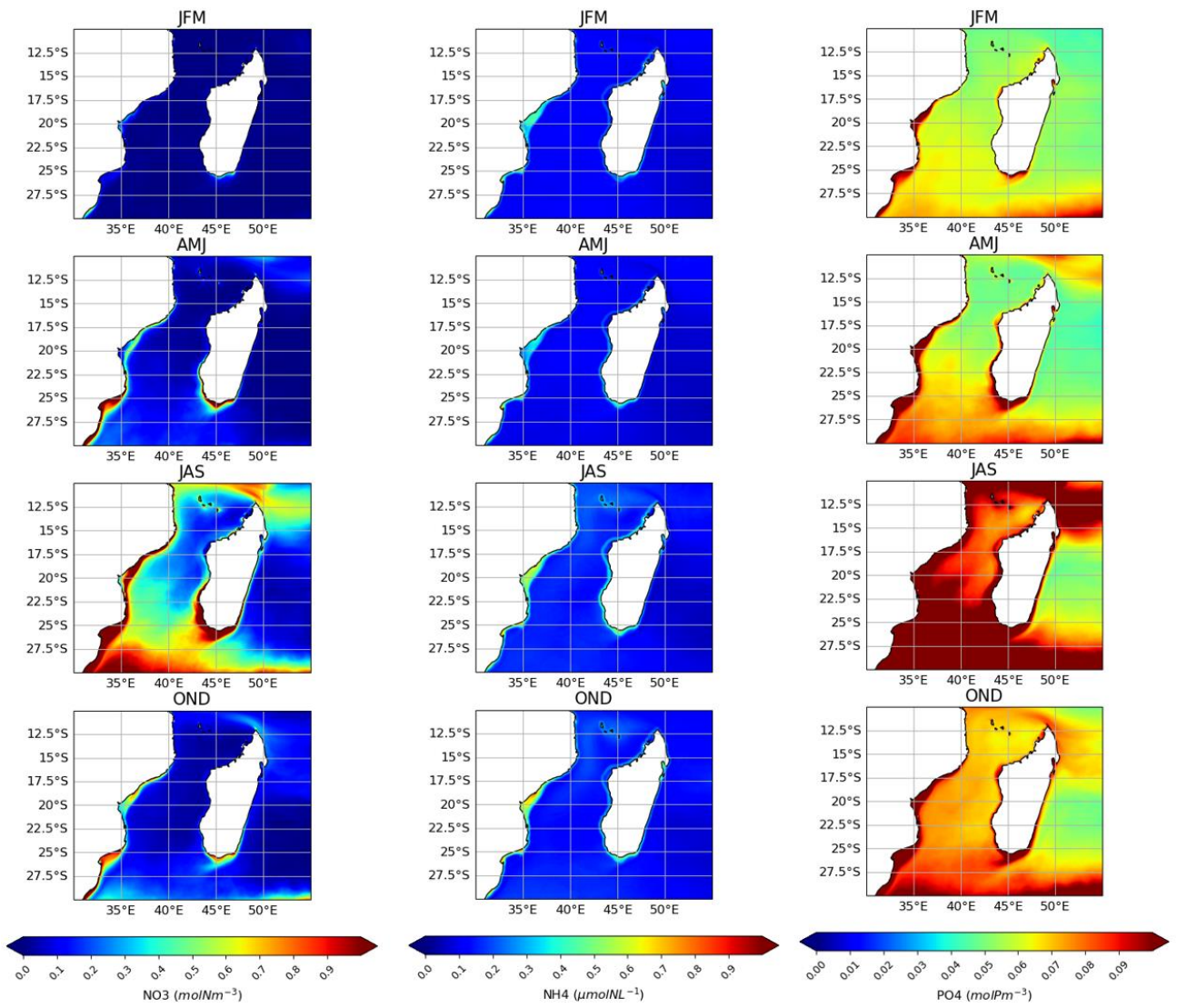


Figure S11. Same as Figure S8 for surface nitrate (left), 0-200m depth-integrated ammonium (middle) and surface phosphate (right).

Si climatology

FER climatology

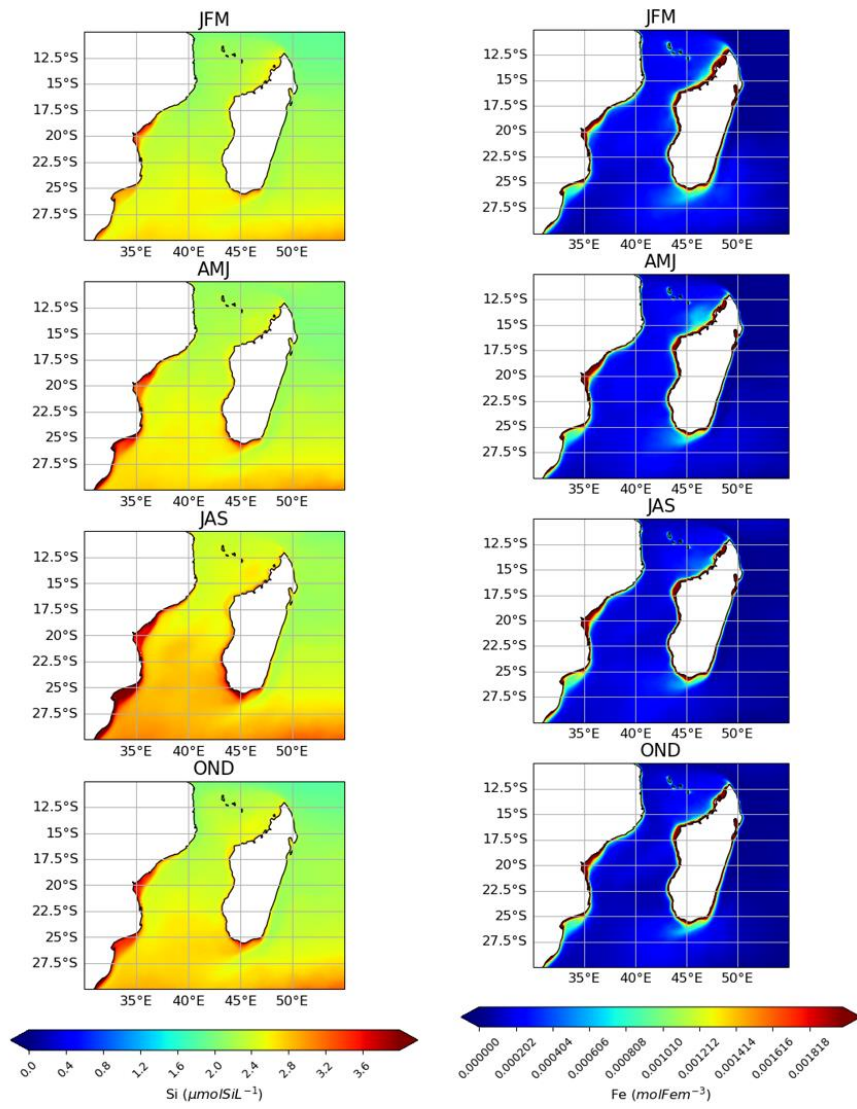


Figure S12. Same as Figure S8 for surface silicate (left), and surface iron (right).

NCHL climatology 0-200m

DCHL climatology 0-200m

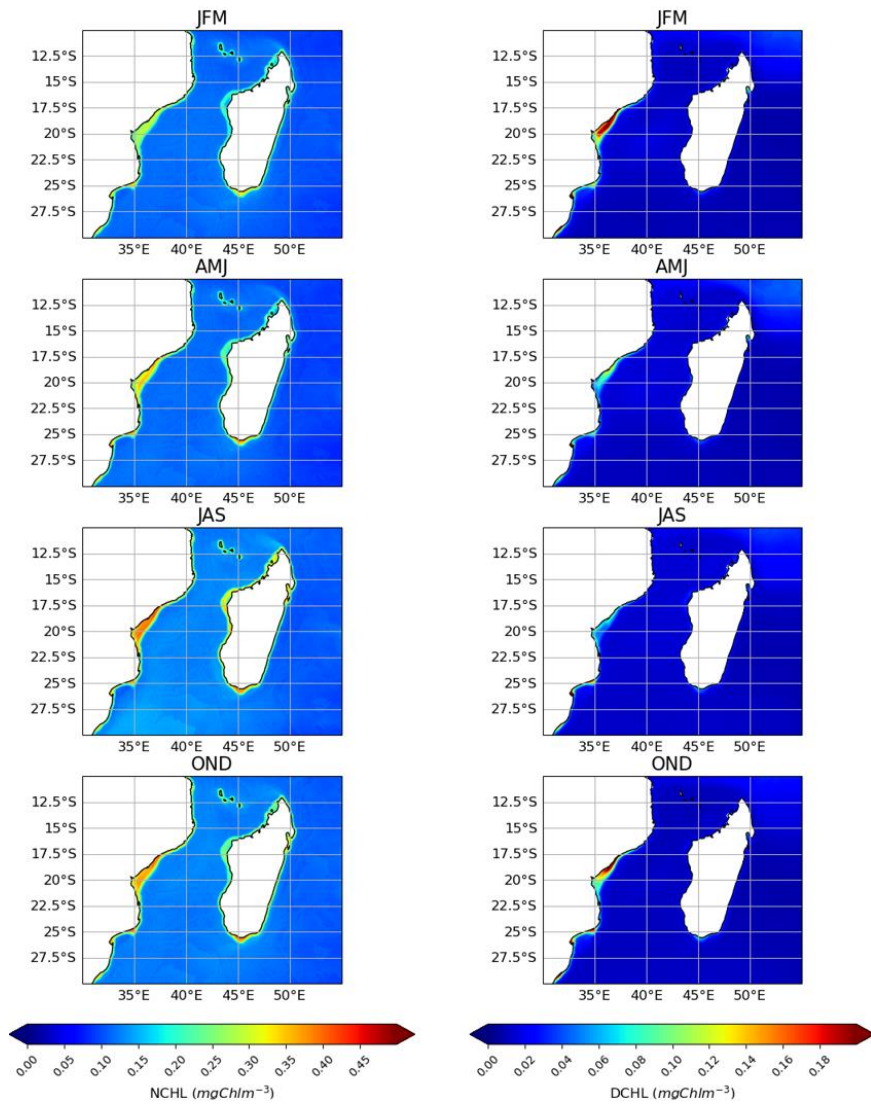


Figure S13. Same as Figure S8 for 0-200m depth-integrated of chlorophyll-a in nanophytoplankton (left) and diatoms (right).

NCHL climatology 0-200m

DCHL climatology 0-200m

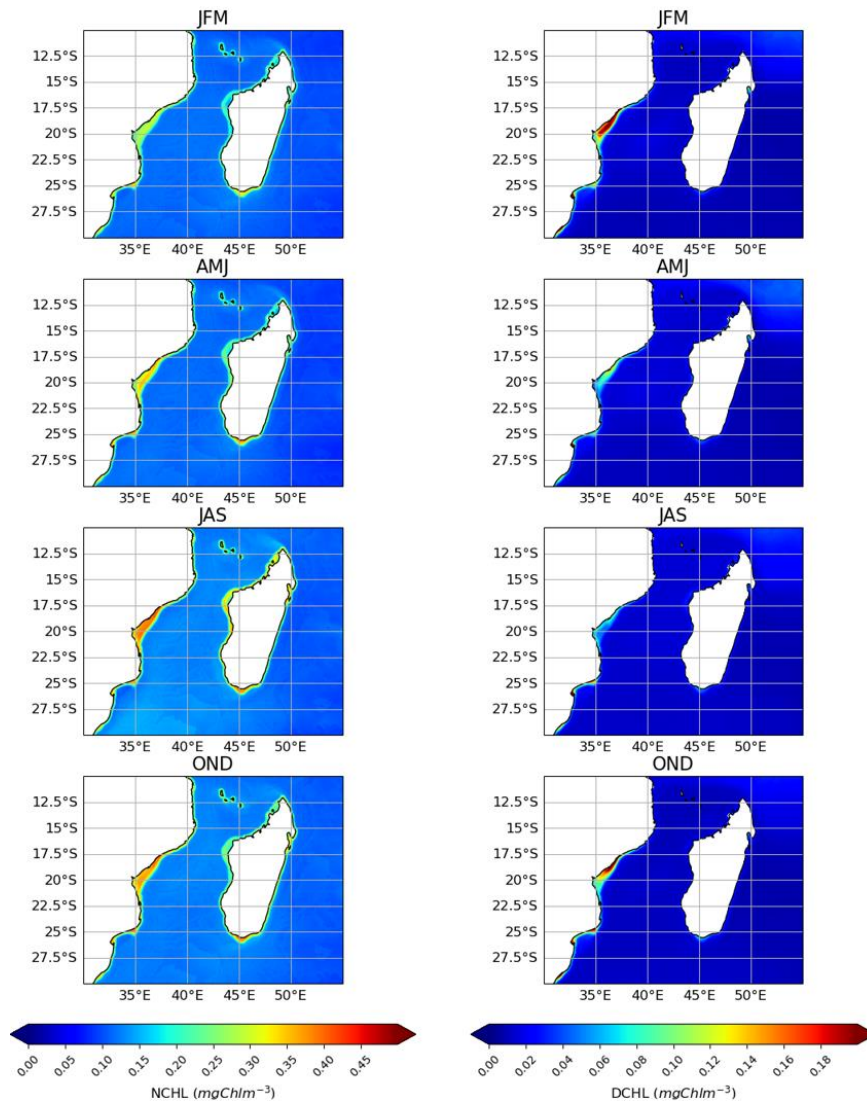


Figure S14. Same as Figure S8 for 0-200m depth-integrated of zooplankton biomass (left) and mesozooplankton biomass (right).

4. Py-eddy-tracker Eddy and parameters used for the eddy detection

Eddy identification was carried out with the py-eddy-tracker python code (Mason et al., 2014). This open-access method was developed based on the method of Chelton et al. (2011) and was previously used to study eddy properties of numerical simulation (e.g., Mason et al., 2017, 2019; Smith and Fortin, 2022) and is used by CMEMS on satellite observations (AVISO, 2016). The py-eddy-tracker seeks the outermost closed contours of SSH. SSH closed shapes are identified at intervals of 2 cm. To discard non-eddy features, a series of tests are applied to each identified closed contour as follows:

- A shape test is performed with an error $\leq 50\%$; the error is defined as the ratio between the surface sum of deviations of the closed contour from its fitted circle and the area of that circle (see Kurian et al., 2011).
- The contour must contain a pixel count, l , satisfying $l_{\min} \leq l \leq l_{\max}$ where $l_{\min}=10$ and $l_{\max}=2000$.
- The contour must contain only pixels with SSH values above (below) the current SSH interval value for anticyclones (cyclones).
- The contour must include only one local SSH extrema: max values refer to anticyclones (AC), and min values refer to cyclones (CC).
- The shape must have amplitude A that satisfies $1 \leq A \leq 150$ cm. A is the absolute difference between SSH at the contour used to define L_{eff} (see below) and the SSH extrema within the closed contour.

The closed contour meeting all those requirements mentioned above is defined as the effective contour (C_{eff}) of a newly identified eddy (solid red line in Figure S12). The associated radius, the effective radius L_{eff} , is estimated as the radius of a circle (red dashed line in Figure S12)- with the same area as the region enclosed by SSH closed contour - with a centroid P_{eff} (as shown with red dashed line and dot in Figure S12). A speed-based contour, C_{spd} , is then defined as the contour with the maximum circum-average geostrophic speed contour, U (the rotational speed of the eddy) within the closed contour of SSH (solid green line in Figure S12). L_{spd} is estimated by iterating from C_{eff} inward overall closed contour that satisfies the pixel count test. The associated centroid of C_{spd} is P_{spd} . In this study, we will consider C_{spd} as the contour of the eddy core limit. Additional parameters are extracted for the eddy tracking,

such as the tracking centroid, P_{trk} , which corresponds to the tracking contour, C_{trk} , of the last iteration (i.e., where I tends toward I_{min}).

Eddy properties, which are saved at each time step, include the position of C_{spd} and C_{trk} (in longitude, latitude), date, effective radius (L_{eff}), speed-based radius (L_{spd}), amplitude (A), and rotational speed (U).

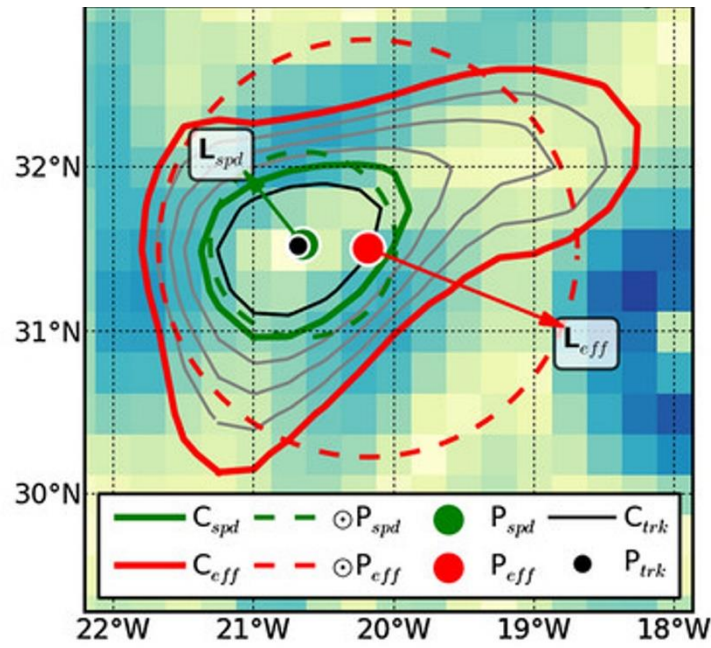


Figure S15: Schematic of the eddy detection method from Mason et al. (2014) as explained in the text. The effective contour C_{eff} , in the solid red line, is the outline of irregularly cyclonic shape eddy, with its associated circle shape, $\odot P_{eff}$, in red dashed line, with an effective radius L_{eff} and a centroid P_{eff} . The speed-based contour parameters, C_{spd} , L_{spd} , P_{spd} , and $\odot P_{spd}$ are shown in green. Gray contours show the remaining contours iterations sampled to identify C_{spd} and, hence, estimate L_{spd} . The black contour, C_{trk} , corresponds to the pixel count lower limit (I_{min}), and P_{trk} , the centroid of this contour, is used for eddy tracking.

References:

- Chelton, D. B., M. G. Schlax, and R. M. Samelson (2011), Global observations of nonlinear mesoscale eddies, *Prog. Oceanogr.*, 91(2), 167–216, doi:10.1016/j.pocean.2011.01.002.
- Mason, E., Pascual, A., & McWilliams, J. C. (2014). A new sea surface height–based code for oceanic mesoscale eddy tracking. *Journal of Atmospheric and Oceanic Technology*, 31(5), 1181-1188.

- Mason E., Pascual A., Gaube P., Ruiz S., Pelegrí J.L., Delepouille A. (2017). Subregional characterization of mesoscale eddies across the Brazil-Malvinas confluence, *J. Geophys. Res.-Oceans*, 122, pp. 3329-3357, 10.1002/2016JC012611
- Mason E., Ruiz S., Bourdalle-Badie R., Reffray G., García-Sotillo M., Pascual A. (2019). New insight into 3-D mesoscale eddy properties from CMEMS operational models in the western mediterranean *Ocean Sci.*, 15, pp. 1111-1131, 10.5194/os-15-1111-2019
- Smith, G.C. and A.S. Fortin (2022), Verification of eddy properties in operational oceanographic analysis systems, *Ocean Modelling*, 172 <https://doi.org/10.1016/j.ocemod.2022.101982>.
- AVISOSsalto/Duacs User Handbook: (M)SLA and (M)ADT Near-Real Time and Delayed Time Products (2016). CLS-DOS-NT-06-034, Issue 5rev0. Mesoscale Eddy Trajectory Atlas Product Handbook, SALP-MU-P-EA-23126-CLS, Issue 3rev2.
- Kurian, J., Colas, F., Capet, X., McWilliams, J. C., & Chelton, D. B. (2011). Eddy properties in the California current system. *Journal of Geophysical Research: Oceans*, 116(C8).

5. The model mesoscale activity and comparison with observations

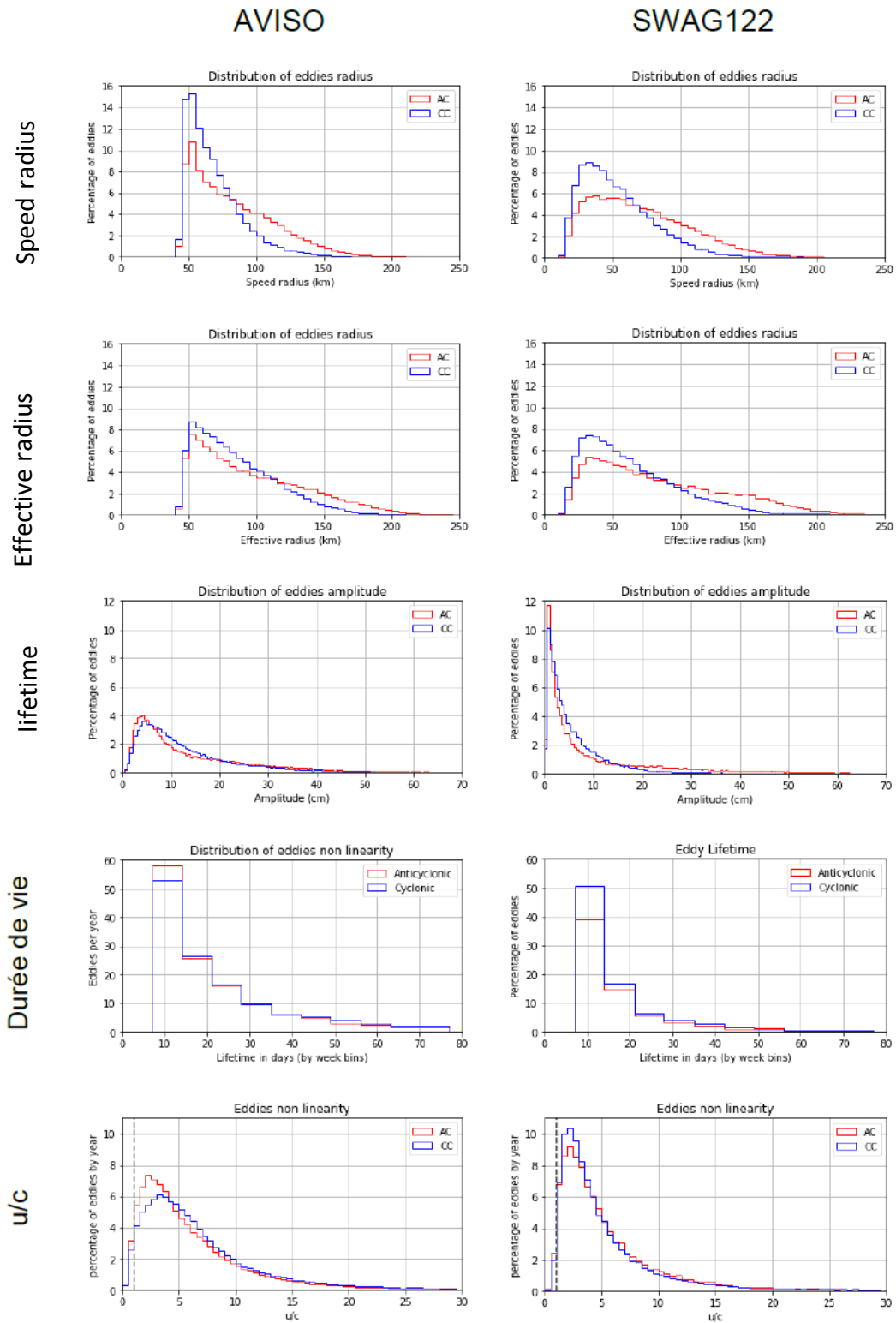


Figure S16. Same as Figure S6 zoomed from 0 to 500m depth.

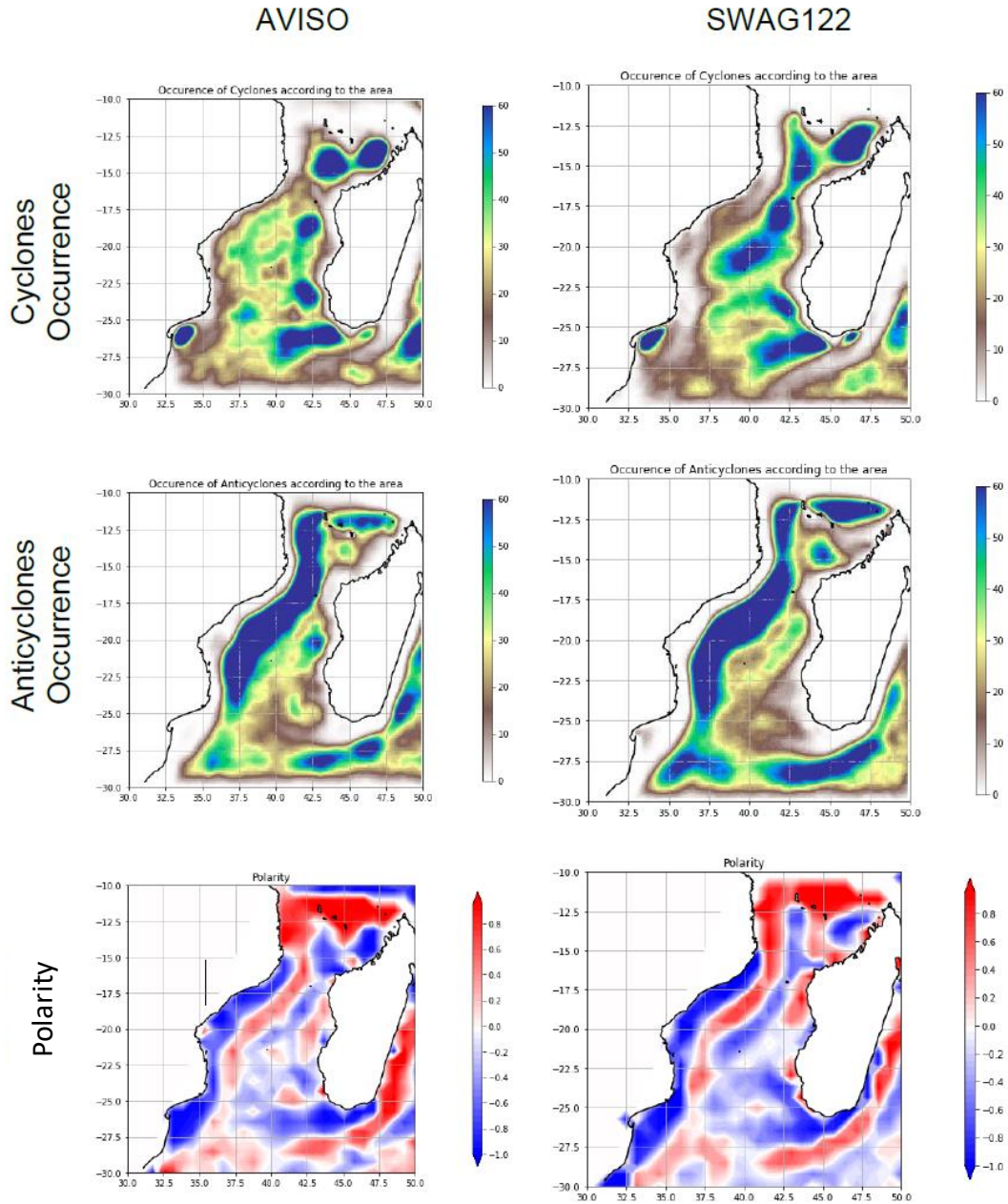


Figure S17. Occurrence and polarity of cyclonic and anticyclonic eddies for AVISO (left), WOES12 (middle) and SWAG122 (right) observations. Eddy polarity highlights the dominance of anticyclones (red) or cyclones (blue). Eddy polarity is calculated as follows: $[(na-nc)/(na+nc)]$, with na and nc the numbers of anticyclones and cyclones, respectively. Regions where $na = 0$ or $nc = 0$ are masked.

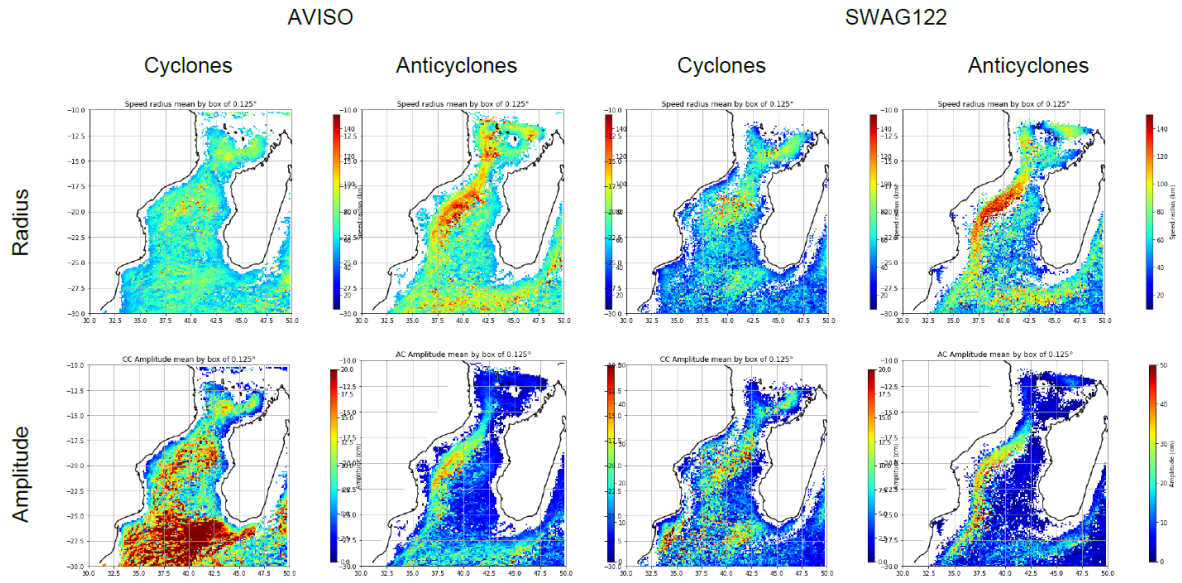


Figure S18. Distribution of radii associated with speed radius (top) and amplitude (bottom) for AVISO (left) and SWAG122 (right).

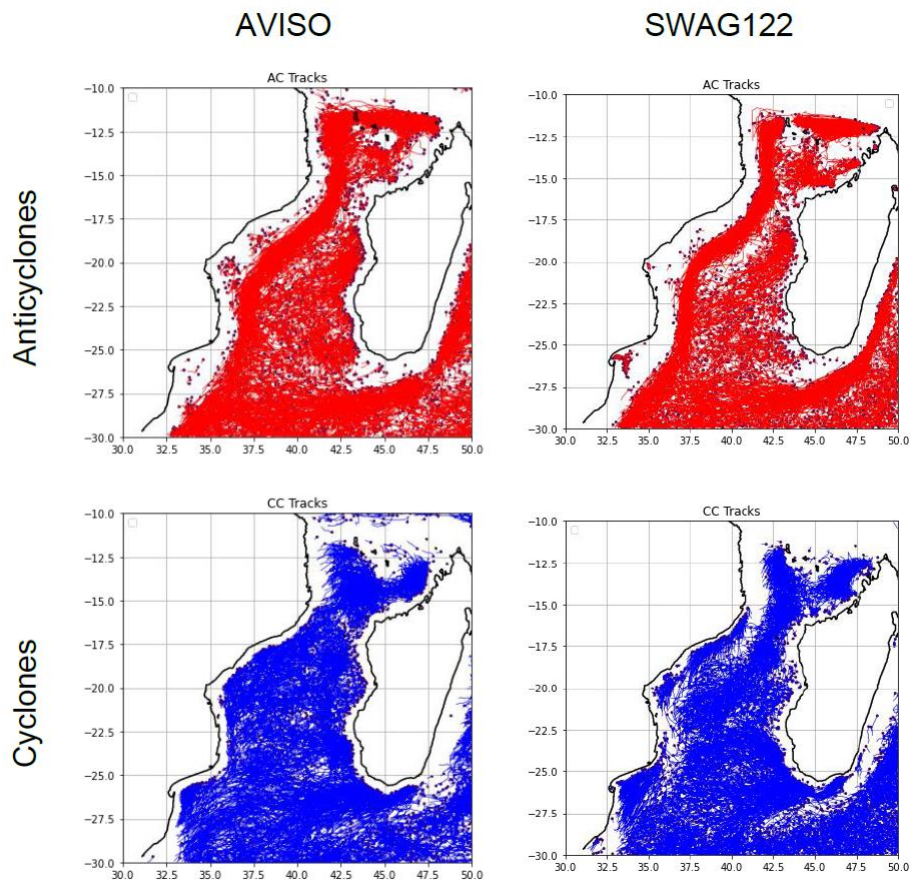


Figure S19. Tracks of anticyclones (in red) and cyclones (in blue) have been plotted for AVISO (on the left) and SWAG122 (on the right). The black dots located at the beginning of the eddy trajectory have been indicated.

6. The Additional analysis

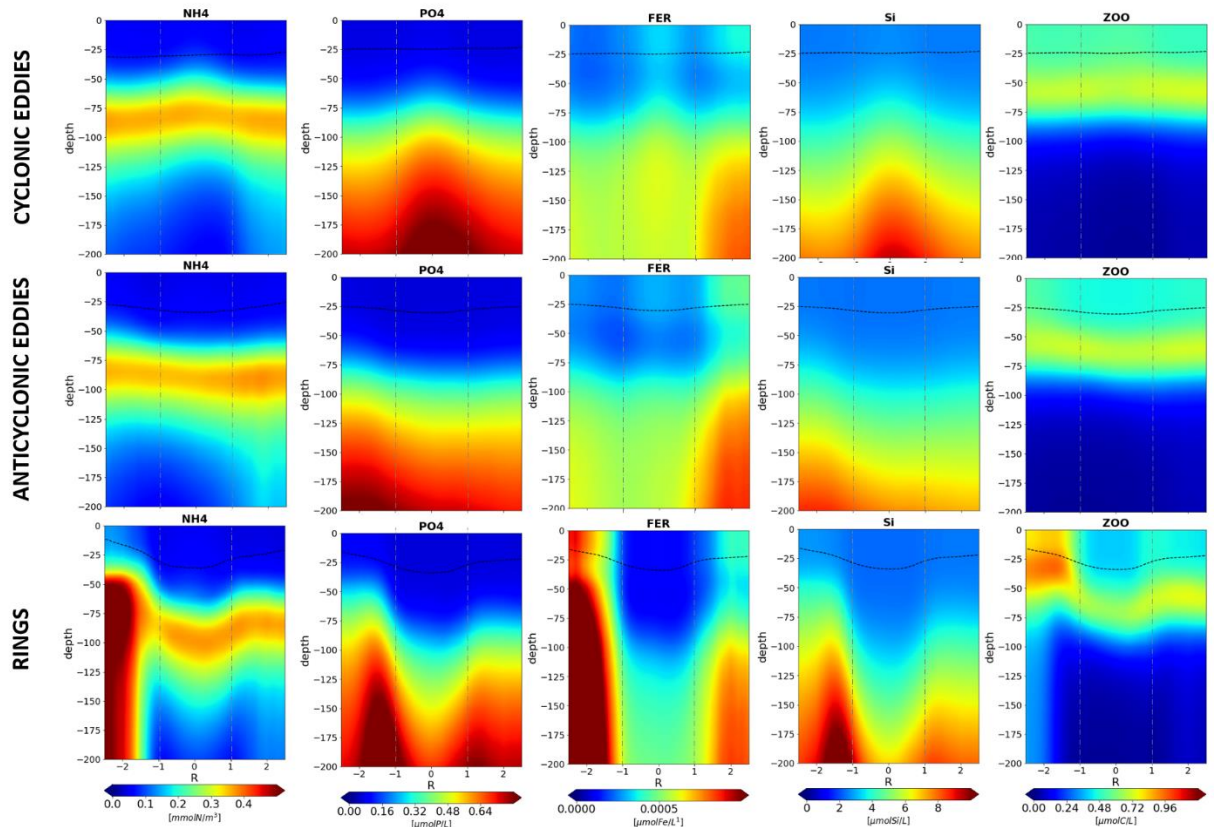
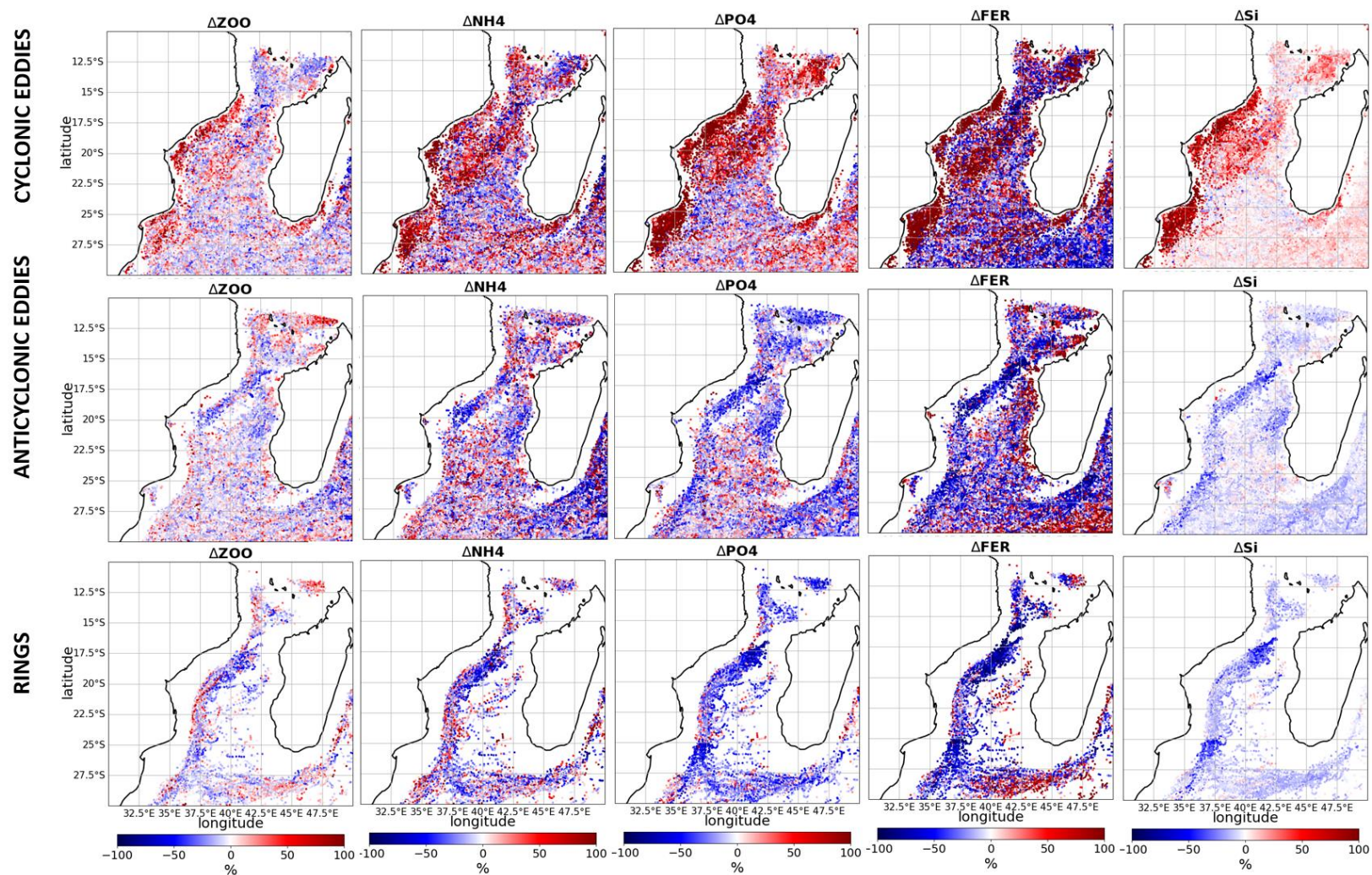
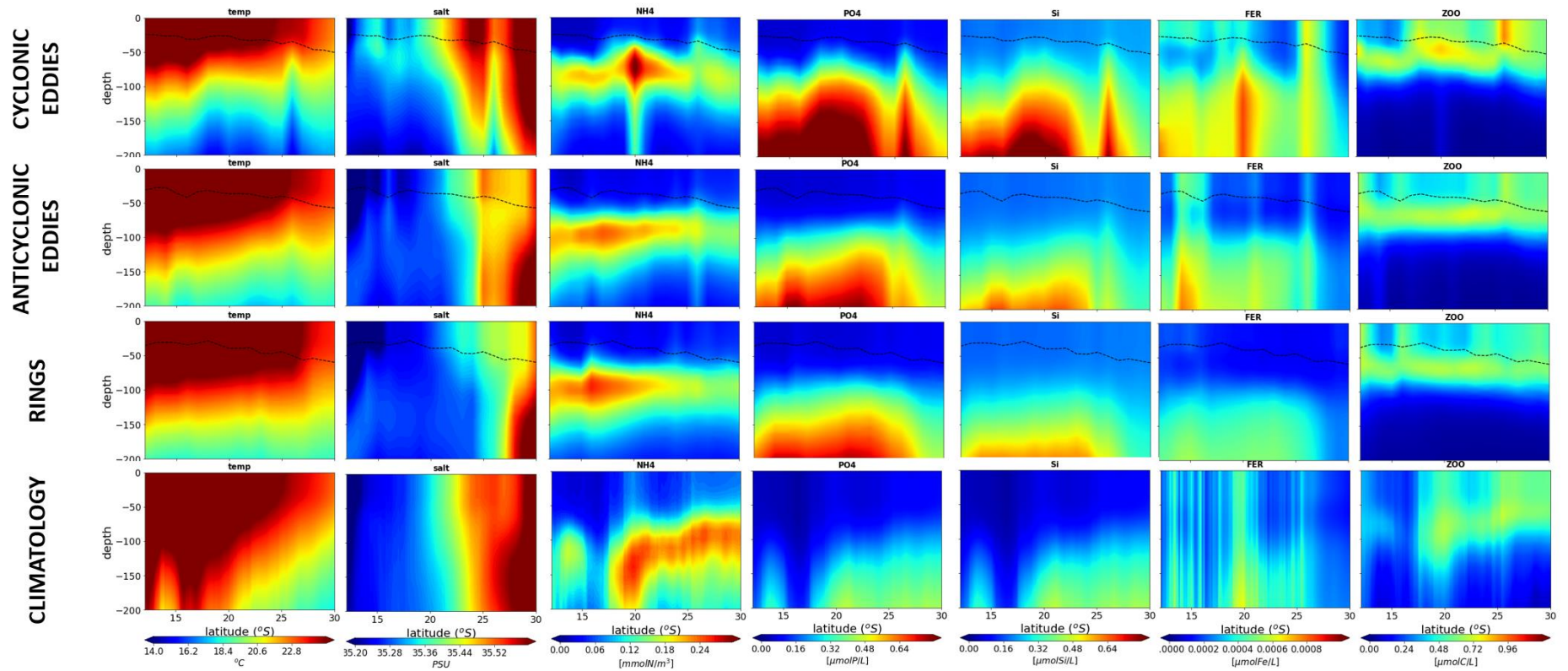


Figure S20. Average properties of (top row) cyclonic eddies, (middle row) anticyclonic eddies - without rings - and (bottom row) rings for eddies between 13.5°S and 20°S. From left to right: ammonium (NH₄), phosphate (PO₄), Iron (Fer), Silicate (Si), and zooplankton (ZOO). The composites represent the average profiles across eddies, with the eddy core centered at 0 and R the radius of the eddy core (positive R represents the eastern side). The dashed line represents the mixed layer depth. Vertical dashed grey lines indicate the eddy core limit ($\pm 1R$).



1

2 **Figure S21.** Anomalies between the eddy core and the area surrounding the eddy, averaged over 100m depth, expressed in percentage, in (top row) cyclonic eddies, (middle row) anticyclonic
 3 eddies, and (bottom row) rings, for zooplankton (ZOO), ammonium (NH₄), phosphate (PO₄), Iron (Fer) and Silicate (Si).



4

5 **Figure S22.** Latitudinal vertical sections of properties in (top row) cyclonic eddy cores, (second row) anticyclonic eddy cores (third row) rings core and (fourth row) for 20-year climatology, averaged

6 across the channel, for temperature, salinity, ammonium (NH₄), phosphate (PO₄), Silicate (Si), Iron (Fe) and zooplankton (ZOO). The dashed line represents the mixed layer depth.